Effect of Interfacial Contact Forces in Lateral Contact Wire Strand

B. K. Gnanavel, N. S. Parthasarathy

Abstract—A new mathematical model has been developed to predict the behaviour of a stranded cable assembly under the influence of interfacial lateral contact forces. A single layered cable assembly with six helical wires and a straight cylindrical core, all made with the same material, steel, has been chosen to explain this phenomenon when the assembly is under the influence of wire – wire lateral contact. An attempt is made in this paper to model the strand with a lateral (wire–wire) contact and deduce its equations of equilibrium. Numerical analysis of strand force, twisting moment, strand stiffness coefficients and contact stresses are carried out based on the equilibrium of thin rods, and the results are compared with the earlier research work and experimental test. The importance of the inclusion of interfacial forces at the contact locations and their associated effects of axial and twist slip of the helical wires on the wire is highlighted. Few results have been reported on the effects of interfacial contact. The behaviour of the stranded cable assembly due to the contact force in the lateral direction is one more additional feature incorporated in the present work.

Index Terms—contact stress, friction, cable mechanics.

I. Introduction

Wire strands are playing a very important role in various engineering applications such as suspension bridges, electrical power transmission lines and pre-stressing of concrete etc., apart from hauling, traction, lifting & other allied mechanical engineering applications. They consist of groups of wires wound over helically together in a regular geometric pattern to form an integral unit to afford axial strength and stiffness. It is well known that a major advantage of such element is their capacity to support large axial loads with comparatively small bending and torsional stiffness.

It is imperative that the nature of the contact that occurs between the wires in the strands is vital to determine their strength, life and also helps to predict the failures, as these interfaces are vulnerable locations during loading & functioning. Three important contact modes occur in a single layered strand. During axial loading of such strands, the wires in the layer, maintain line contact among themselves and also with the central core, on which they are wound. This is called the combined contact mode. Depending on the geometrical constructions like the diameter, helix of the wires in the outer layer strand and the diameter of the inner core and the differential contraction between the core and the wires, the contact mode may shift to that among the wires in the layer only. This is called the lateral contact mode and in such case, the central core loses the contact with the outer wires and the contact stresses in the helical wire interfaces only exist. In wire rope applications, such contact mode is generally desired upon, as the central core is made up of hemp or fibrous material, offering more flexibility in working on a drum or sheave pulleys/shackles. In the third mode of contact, called as core-wire contact, the helical wires in the layer loose contact among themselves and retain contact only with the core. This paper focuses the mechanism that occurs in a lateral contact mode on a single layered metallic wired strand with a central core of the same material.

Love [1] outlines the basic formulations of the theory of thin rods under bending & torsional loads that form the mathematical basis for such stranded cables. Costello & Phillips [2, 3] have made significant contributions to explain the contact mechanisms of cables under lateral contact mode and have derived expressions for the contact forces that occur in the wire interfaces. The same authors in their further works [4& 5] presented more exact expressions for the contact angle and also predicted the effective modulus of the twisted wire cables in the lateral contact mode. Costello & Sinha [6] investigated the torsional stiffness of a single layered wired strand in the lateral contact mode. The above findings and the mathematical relations concerned with the mechanics of wires of stranded cables under different modes of contact have been reported in detail by Costello [7] in his book. Kumar et al [8] have summarised the analytical expressions reported by the above authors to explain the phenomenon of combined tension and torsion loadings and derived expressions for the contact stresses in such cables. All the literature mentioned above have independently handled one or the other mode of contact with or without the presence of a metallic core or with fibrous core. In reality, in stranded cables under loading, none of these contact modes occur in isolation to consider as though that only exists. Depending on the geometry like diameters , helix angle , the extent of contraction of the wires and the core that prevail during each stage of loading , the contact mode changes from one to the other and hence knowledge of the mechanics connected with each of these modes become important. Gnanavel et al [9] have presented an analytical model to explain the importance of the interfacial loads and their effects in coupled contact and identified the threshold limit at which the contact mode changes from a coupled arrangement to the arrangement of core-wire radial contact and analysed further a radial contact mode in their works

* Professor of Mechanical Engineering, Department of Mechanical Engineering, Saveetha Engineering College, Saveetha Nagar, Saveetha Nagar, Thandalam, Chennai - 602105, Tamilnadu, India. email: bkgnanavel@yahoo.com
** Professor of Mechanical Engineering, Department of Mechanical Engineering, MVJ College of Engineering, Channasandra, Bangalore – 560 067, Visvesvaraya Technological University, Karnataka,India, parthan.nsp@gmail.com

ISBN: 978-988-19251-5-2
ISSN: 2078-0958 (Print); ISSN: 2078-0966 (Online)

[10]. However these works were confined to a coupled and radial contact mode single straight cored helical strand.

The present paper presents exclusively the lateral contact mode modelling with its complete analytical development in the lines of the above authors but considers the effect of the frictional forces at the contact interface, hitherto not considered fully. The effect of the distributed contact force in the normal direction and their association in the tangential directions due to friction are the significant contributions of this paper. Further, the interaction of the distributed moments in the normal and axial (tangential) direction of the helical wires and their effects in the response of the cables are the distinct features of this work. Consideration of all these parameters brings out expressions for the wire force in the normal direction, which was generally treated as zero by the other investigators. Detailed experimental work has also been carried out in one of the research laboratories dealing with cables used for electrical power transmission.

II. Analytical Formulation of the Lateral Contact in a Seven Wire Strand

In the following analysis, each wire is considered in the strand as a long slender curved rod. Figures 1 and 2 depict the cross section and the developed geometry of a seven wire strand, in the lateral contact. The forces and moments that act in the helical wires along the normal, binormal and tangential directions are as shown in Figure 3. The components of the force resultant acting on the cross section of the wire are denoted by *N*, *N'*, *T* and the components of moment acting on the cross section are denoted by *G*, *G'*, *H*. The components of the distributed force per unit length of the wire are *X*, *Y* and *Z* and the components of the distributed moment per unit length of the wire are *K*, *K'* and *Θ*. Along any line of contact between the helical wires, there exists the normal distributed force *U* and the tangential distributed forces *V* and *W* as shown in Figure 4.

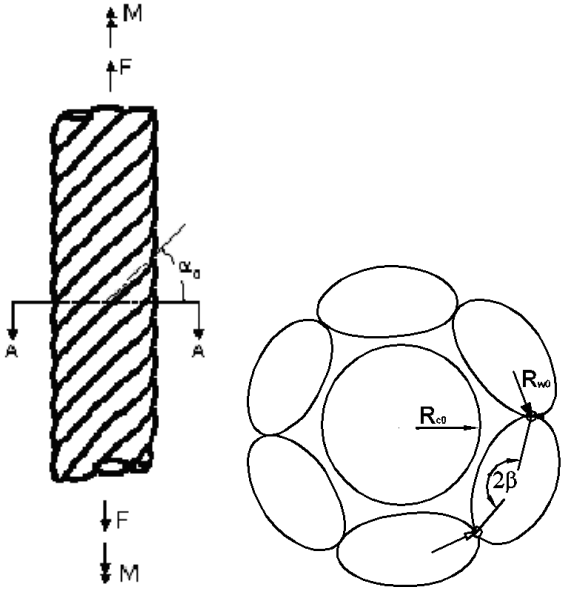

Fig. 1 Strand geometry

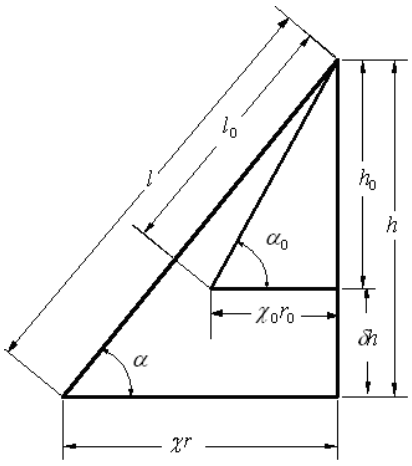

Fig. 2 Wire helix geometry

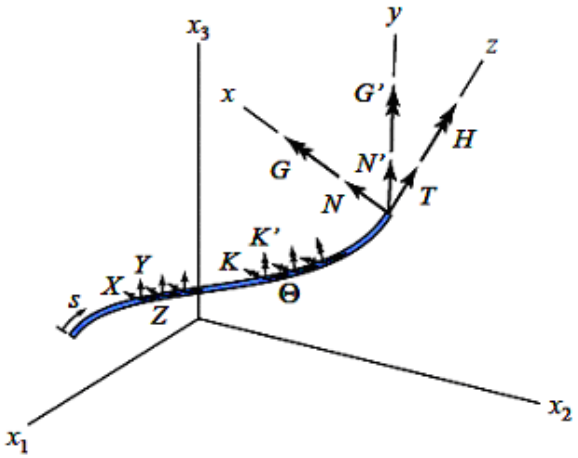

Fig. 3 Forces and moments on a helical wire

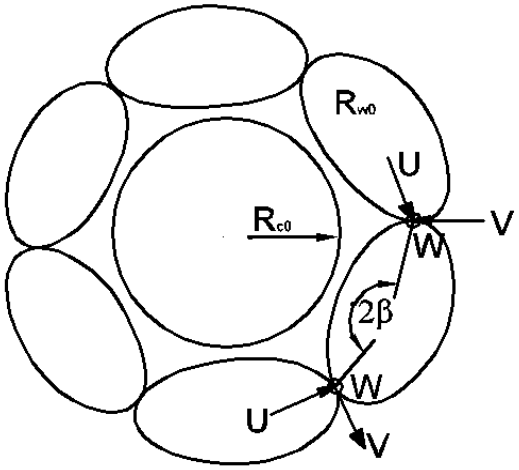

Fig. 4 Distributed loads on a helical wire

The above interfacial forces can be related to the forces and moments in the normal, binormal and tangential directions of the wire, as under:

$$X = -2U\cos\beta,\ Y = 2V\cos\beta,\ Z = 0 \quad (1)$$

$$K = 2WR_{w0}\sin\beta,\ K' = 0,\ \Theta = 2VR_{w0} \quad (2)$$

where R_{w0} is the radius of the wire, β is the contact angle, which locates the lines of action of the line contact loads *U* on a wire due to its adjacent wires. The contact angle can be determined from the intersection of the projection of the cross section and the projection of the line of contact.

ISBN: 978-988-19251-5-2
ISSN: 2078-0958 (Print); ISSN: 2078-0966 (Online)

Costello et al (1974) derived the expressions for the contact angle as given by

$$\cos\beta = \frac{1}{\cos^2\alpha_0}\left[\sqrt{1+\frac{\tan^2\left(\frac{\pi}{2}-\frac{\pi}{m}\right)}{\sin^2\alpha_0}} - \sqrt{\tan^2\left(\frac{\pi}{2}-\frac{\pi}{m}\right)\left(1+\frac{1}{\tan^2\alpha_0\cos^2\left(\frac{\pi}{2}-\frac{\pi}{m}\right)\left(\sin^2\alpha_0+\tan^2\left(\frac{\pi}{2}-\frac{\pi}{m}\right)\right)}\right)+\sin^4\alpha_0}\right] \quad (3)$$

where m is the number of wires in that layer, α_0 is the helix angle.

The equations of equilibrium of all the forces and the moments acting on an infinitesimal element of the wire are obtained from the theory of slender curved rods by Love [1]. Since the strand is considered long, all the derivatives of stress resultants and moments with respect to the arc length of the wire are neglected. Since the helical wire is wound on a straight cylindrical core, the normal curvature and the associated normal bending moment of the wire are zero. Hence, the equations of equilibrium are written as,

$$-N'\tau_0 + T\kappa_0' + X = 0 \quad (4)$$

$$N\tau_0 + Y = 0 \quad (5)$$

$$-N\kappa'_0 + Z = 0 \quad (6)$$

$$-G'\tau_0 + H\kappa_0' - N' + K = 0 \quad (7)$$

$$N + K' = 0 \quad (8)$$

$$\Theta = 0 \quad (9)$$

where κ'_0 is the binormal curvature and τ_0 is the twist of the wire.

The principal binormal curvature and twist of the centre line of the wire are given by,

$$\kappa_0' = \frac{\cos^2\alpha_0}{r_0} \quad (10)$$

$$\tau_0 = \frac{\cos\alpha_0\sin\alpha_0}{r_0} \quad (11)$$

where r_0 is the helix radius.

The helix radius in the lateral contact mode as derived by Costello [6] is given by

$$r_0 = R_{w0}\sqrt{1+\frac{\tan^2\left(\frac{\pi}{2}-\frac{\pi}{m}\right)}{\sin^2\alpha_0}} \quad (12)$$

When the slipping between helical wires during the extension of the strand is considered, the tangential distributed forces at the wire interfaces are given by,

$$V=\mu U\ ;\ W=\mu U \quad (13)$$

where μ is the coefficient of friction between the wire - wire.

Combining Equation (13) with the above mentioned equations, the wire force in the normal and binormal directions are respectively are obtained as follows:-

$$N = G'\left[\frac{\tau_0}{(\kappa_0'-\tau_0)R_{0w}\sin\beta}\right] - H\left[\frac{\kappa_0}{(\kappa_0'-\tau_0)R_{0w}\sin\beta}\right] + N'\left[\frac{\cos\beta}{(\kappa_0'-\tau_0)R_{0w}\sin\beta}\right] \quad (14)$$

$$N' = -G'\left[\frac{\left(\frac{\tau_0}{R_{w0}(\kappa_0'-\tau_0)\sin\beta}\right)-\left(\frac{\tau_0\cos\beta}{\mu R_{w0}\sin\beta}\right)+\left(\frac{\tau_0}{\cos\beta}\right)}{\left(\frac{\cos\beta}{R_{w0}(\kappa_0'-\tau_0)\sin\beta}\right)-\tau_0-\left(\frac{\cos\beta}{\mu R_{w0}\sin\beta}\right)+\left(\frac{1}{\sin\beta}\right)}\right] - H\left[\frac{\left(\frac{\kappa_0'\cos\beta}{\mu R_{w0}\sin\beta}\right)-\left(\frac{\kappa_0'}{R_{w0}(\kappa_0'-\tau_0)\sin\beta}\right)+\left(\frac{\kappa_0'}{\sin\beta}\right)}{\left(\frac{\cos\beta}{R_{w0}(\kappa_0'-\tau_0)\sin\beta}\right)-\tau_0-\left(\frac{\cos\beta}{\mu R_{w0}\sin\beta}\right)+\left(\frac{1}{\sin\beta}\right)}\right] - T\left[\frac{\kappa_0'}{\left(\frac{\cos\beta}{R_{w0}(\kappa_0'-\tau_0)\sin\beta}\right)-\tau_0-\left(\frac{\cos\beta}{\mu R_{w0}\sin\beta}\right)+\left(\frac{1}{\sin\beta}\right)}\right] \quad (15)$$

The axial forces in the wire, bending moment in the binormal direction and twisting moment of the wire are found by the following relations:-

$$T = E\pi R_{w0}^2\varepsilon_w \quad (16)$$

$$G' = \frac{E\pi R_{w0}^4}{4}\Delta\kappa' \quad (17)$$

$$H = \frac{E\pi R_{w0}^4}{4(1+\nu)}\Delta\tau \quad (18)$$

where E is the Young's modulus, ν is the Poisson's ratio, ε_w is the wire axial strain, $\Delta\kappa'$ is the change in binormal curvature and $\Delta\tau$ is the change in twist. The wire axial strain, change in binormal curvature and the change in twist are used as given by Gnanavel et al [10]

The resultant axial force and the axial twisting moment acting on the outer layers of the strand are given by,

$$F_w = m\left(T\sin\alpha_0 + N'\cos\alpha_0\right) \quad (19)$$

$$M_w = m\left[\left(H\sin\alpha_0\right)+\left(G'\cos\alpha_0\right)+\left(Tr\cos\alpha_0\right)-\left(N'r\sin\alpha_0\right)\right] \quad (20)$$

The axial force F_c and the axial twisting moment M_c acting on the centre core are given by the expressions

$$F_c = E\pi R_{c0}^2\varepsilon \quad (21)$$

$$M_c = \frac{E\pi R_{c0}^4}{4(1+\nu)}\left(\frac{d\chi}{h}\right) \quad (22)$$

where R_{c0} is the core radius, ε is the strand axial strain, $\left(\frac{d\chi}{h}\right)$ is the strand angle twist per unit length,

The total axial force F and the total twisting moment M acting on the strand can be written as

$$F = F_c + F_w \quad (23)$$

$$M = M_c + M_w \quad (24)$$

The above expressions can also be expressed in terms of strand axial strain, ε and angle of twist per unit length strand, $(d\chi/h)$ as follows

$$\begin{Bmatrix} F \\ M \end{Bmatrix} = \begin{bmatrix} F_\varepsilon & F_\chi \\ M_\varepsilon & M_\chi \end{bmatrix}\begin{Bmatrix} \varepsilon \\ \frac{d\chi}{h} \end{Bmatrix} \quad (25)$$

where F_ε, F_χ, M_ε and M_χ are the stiffness coefficients of the strand. On substitution of the equations 14 to 18 and rearranging, the following stiffness constants are obtained.

$$F_\varepsilon = E\pi R_{c0}^2 + a\sin\alpha_0 + eg\cos\alpha_0 + ch\cos\alpha_0 + ai\cos\alpha_0 \quad (26)$$

$$F_\chi = b\sin\alpha_0 + fg\cos\alpha_0 + dh\cos\alpha_0 + bi\cos\alpha_0 \quad (27)$$

ISBN: 978-988-19251-5-2
ISSN: 2078-0958 (Print); ISSN: 2078-0966 (Online)

$$M_{\varepsilon} = c\sin\alpha_0 + e\cos\alpha_0 + ar\cos\alpha_0 - egr\sin\alpha_0 - chr_0\sin\alpha_0 - air\sin\alpha_0 \quad (28)$$

$$M\chi = \frac{E\pi R_{c0}^4}{4(1+\nu)} + d\sin\alpha_0 + f\cos\alpha_0 + br\cos\alpha_0 - fgr\sin\alpha_0 - dhr_0\sin\alpha_0 - bir\sin\alpha_0 \quad (29)$$

where,

$$a = E\pi R_{w0}^2\left[\frac{\tan^2\alpha_0 - \left(\frac{\nu R_{c0}}{r_0}\right)}{1+\tan^2\alpha_0 + \left(\frac{\nu R_{w0}}{r_0}\right)}\right];$$

$$b = E\pi R_{w0}^2\left[\frac{r_0\tan\alpha_0}{1+\tan^2\alpha_0 + \left(\frac{\nu R_{w0}}{r_0}\right)}\right]$$

$$c = \frac{E\pi R_{w0}^4}{2}\left\{\left[\left(\frac{\tan\alpha_0}{r_0}\right) - \left(\frac{2\sin^2\alpha_0\tan\alpha_0}{r_0}\right) + \left(\frac{\nu R_{c0}\sin\alpha_0\cos\alpha_0}{r_0^2}\right)\right] + \left[-\left(\frac{\tan\alpha_0}{r_0}\right) + \left(\frac{2\sin^2\alpha_0\tan\alpha_0}{r_0}\right) + \left(\frac{\nu R_{w0}\sin\alpha_0\cos\alpha_0}{r_0^2}\right)\right]\left[\frac{\tan^2\alpha_0 - \left(\frac{\nu R_{c0}}{r_0}\right)}{1+\tan^2\alpha_0 + \left(\frac{\nu R_{w0}}{r_0}\right)}\right]\right\}$$

$$d = \frac{E\pi R_{w0}^4}{2}\left\{\left[-\left(\frac{\tan\alpha_0}{r_0}\right) + \left(\frac{2\sin^2\alpha_0\tan\alpha_0}{r_0}\right) + \left(\frac{\nu R_{w0}\sin\alpha_0\cos\alpha_0}{r_0^2}\right)\right]\left[\frac{r_0\tan\alpha_0}{1+\tan^2\alpha_0 + \left(\frac{\nu R_{w0}}{r_0}\right)}\right]\right\}$$

$$e = \frac{E\pi R_{w0}^4}{4}\left\{\left[-\left(\frac{2\sin^2\alpha_0}{r_0}\right) + \left(\frac{\nu R_{c0}\cos^2\alpha_0}{r_0^2}\right)\right] + \left[\left(\frac{2\sin^2\alpha_0}{r_0}\right) + \left(\frac{\nu R_{w0}\cos^2\alpha_0}{r_0^2}\right)\right]\left[\frac{\tan^2\alpha_0 - \left(\frac{\nu R_{c0}}{r_0}\right)}{1+\tan^2\alpha_0 + \left(\frac{\nu R_{w0}}{r_0}\right)}\right]\right\}$$

$$f = \frac{E\pi R_{w0}^4}{4}\left\{\left[\left(\frac{2\sin^2\alpha_0}{r_0}\right) + \left(\frac{\nu R_{w0}\cos^2\alpha_0}{r_0^2}\right)\right]\left[\frac{r_0\tan\alpha_0}{1+\tan^2\alpha_0 + \left(\frac{\nu R_{w0}}{r_0}\right)}\right]\right\}$$

$$g = \left[\frac{\left(\frac{\tau_0}{R_{w0}(\kappa_0'-\tau_0)\sin\beta}\right) - \left(\frac{\tau_0\cos\beta}{\mu R_{w0}\sin\beta}\right) + \left(\frac{\tau_0}{\cos\beta}\right)}{\left(\frac{\cos\beta}{R_{w0}(\kappa_0'-\tau_0)\sin\beta}\right) - \tau_0 - \left(\frac{\cos\beta}{\mu R_{w0}\sin\beta}\right) + \left(\frac{1}{\sin\beta}\right)}\right]$$

$$h = \left[\frac{\left(\frac{\kappa_0'\cos\beta}{\mu R_{w0}\sin\beta}\right) - \left(\frac{\kappa_0'}{R_{w0}(\kappa_0'-\tau_0)\sin\beta}\right) + \left(\frac{\kappa_0'}{\sin\beta}\right)}{\left(\frac{\cos\beta}{R_{w0}(\kappa_0'-\tau_0)\sin\beta}\right) - \tau_0 - \left(\frac{\cos\beta}{\mu R_{w0}\sin\beta}\right) + \left(\frac{1}{\sin\beta}\right)}\right]$$

$$i = \left[\frac{\kappa_0'}{\left(\frac{\cos\beta}{R_{w0}(\kappa_0'-\tau_0)\sin\beta}\right) - \tau_0 - \left(\frac{\cos\beta}{\mu R_{w0}\sin\beta}\right) + \left(\frac{1}{\sin\beta}\right)}\right]$$

The movement of the wires along the lines of contact occur depending on the resisting friction force developed at the interface. From equations (4) & (1), the resultant force due to contact in the lateral contact mode is given by,

$$U = \frac{G'\tau_0}{2\mu R_{w0}\sin\beta} - \frac{H\kappa_0}{2\mu R_{w0}\sin\beta} + \frac{N'}{2\mu R_{w0}\sin\beta} \quad (30)$$

The maximum normal contact stresses at the wire interfaces are obtained using Hertzian theory and presented as under.

$$\sigma_{w-w} = \sqrt{\frac{EU\left[\left(\frac{1}{R_{w0}}\right) + \left(\frac{1}{R_{wo}}\right)\right]}{\left[2\pi\left(1-\nu^2\right)\right]}} \quad (31)$$

A. Numerical Example

A stranded cable comprising a layer of six wires wound around a central core is considered to explain the lateral contact arrangement and its effects. The core and the helical wires are chosen with the same material steel with Young's modulus of elasticity as 2×10^5 N/mm^2. An arrangement of an earth wire used in electrical power transmission lines is chosen for the study and that consists of six helical wires of radius 3.5 mm wound around a central core of radius 3.5 mm.

Numerical computations are carried out for a lay ratio of 18.48 of the cable considered. The lay ratio is defined as the ratio between the axial lengths (pitch) of a complete turn of the helix formed by a helical wire in a strand to the external diameter of strand and has been usually maintained as a geometric reference parameter to describe cables and overhead transmission line conductors as per International standards. Since the lay ratio is a geometrical parameter connecting the helix angle of the wire, a lay ratio of 18.48 yielded a helix angle of 83.5º. The above geometry has yielded lateral contact mode as given by equation (12). To explain the behaviour of the cable due to radial contraction and the interfacial friction forces, a Poisson's ratio 0.3 and a friction coefficient of 0.5 have been used in the present work. Since the stranded cable assembly used is an earth wire in overhead transmission applications, it is non-lubricated and generally follows Coulomb's law of friction

ISBN: 978-988-19251-5-2
ISSN: 2078-0958 (Print); ISSN: 2078-0966 (Online)

on dry surface, and hence a coefficient friction of 0.5 has been used.

B. Experimental Work

The experimental setup consists of a test rig of 40 m span with the end fixtures to support a cable and exert a pulling force up to 100 kN. A double acting hydraulic actuator of 100 kN capacity was used to impart the tensile force in the strand. Figure 5(a) shows the hydraulic actuator and Figure (5b) shows the end fixture arrangement. To measure the mechanical response of earth wire strand specimens, a force transducer, and a dial gauge are used as shown Figures (5c & 5d). The strand specimen is 11000 mm in length and is clamped by two sockets at its ends. A dial gauge set up is mounted at the centre of the earth wire strand as shown in Figure 5d and the axial extension of the cable is measured. The least count of the dial gauge is ±0.01 mm. The measurement procedure as recommended by Bureau of Indian Standards (BIS) has been adopted.

Fig. 5a Tensile testing machine

Fig. 5b Tensile testing machine – RHS

Fig. 5c Tensile testing machine – LHS

Fig. 5d Dial gauge mounting with test specimen

C. Comparison of Analytical Models and Experimental Test

Using the numerical data of the strand given above, the results of strand stiffness coefficients, strand axial force, strand twisting moment and contact stress are obtained for the fixed end condition. In the fixed end condition, there is no rotational strain on the strand. The results of the present model are compared with the experimental work and that of Costello model [7]. The variations in the above results are shown as a function of strand axial strain in Figures 6 to 12. Figure 6 is establishing the axial stiffness coefficient as a function of the strand axial strain. Axial stiffness coefficient registers no deviation between of results of the present model and Costello model. The effect of interfacial force has not affected the axial response in the lateral contact mode. However these results are 5.4% greater than the experimental value. Figure 7 shows the tension – torsion coupling stiffness coefficient of the present model and Costello model. The present model estimates 4.6% greater than that of the Costello model. Figure 8 explains the torsional – tension coupling stiffness coefficient of the present model and Costello model. The present model torsion - tension coupling stiffness coefficient is 5.9% less than the Costello model. Figure 9 shows the strand torsional stiffness coefficient of the present model and Costello model respectively. The present model registers an 1.1% increase than the Costello model. Figure 10 explains the strand axial force response of the present model, Costello model and

ISBN: 978-988-19251-5-2
ISSN: 2078-0958 (Print); ISSN: 2078-0966 (Online)

experimental test. The present model and Costello model register same values but are 4.8% less than the experimental results. The strand twisting moment of the cable is shown in Figure 11. The present model predicts an increase of 1.1% than the Costello model. Figure 12 shows the distribution of the contact stresses of the present model and Costello model. However there is no deviation of the results in both the models. The deviation in the results of the above parameters between the present model and the Costello model are due to the inclusion of the frictional effects at the lateral con tact interfaces, their associated distributed moments about the normal and the axial direction of the helical wires. Though the axial response has not shown a difference between the present model and the Costello model, the change of results of the individual parameters are expected to play a significant role in estimating the energy dissipation of such cables.

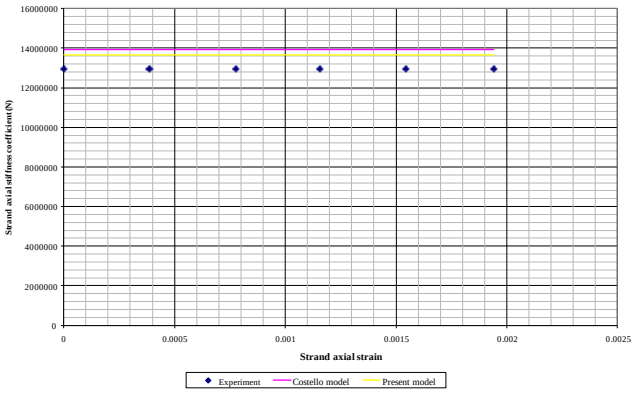

Fig. 6 Strand axial stiffness coefficient

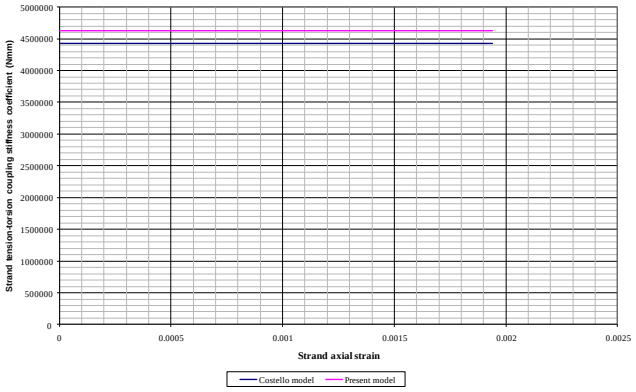

Fig. 7 Strand tension – torsion coupling stiffness coefficient

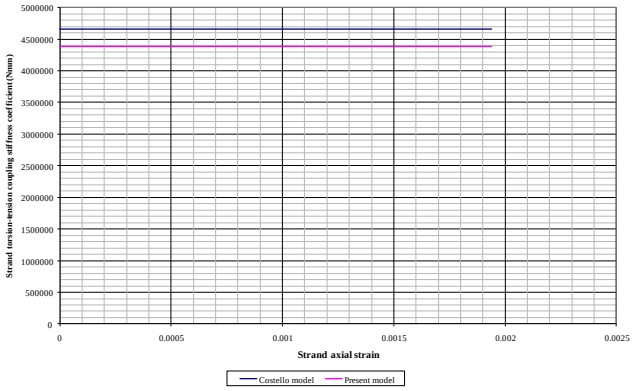

Fig. 8 Strand torsion – tension coupling stiffness coefficient

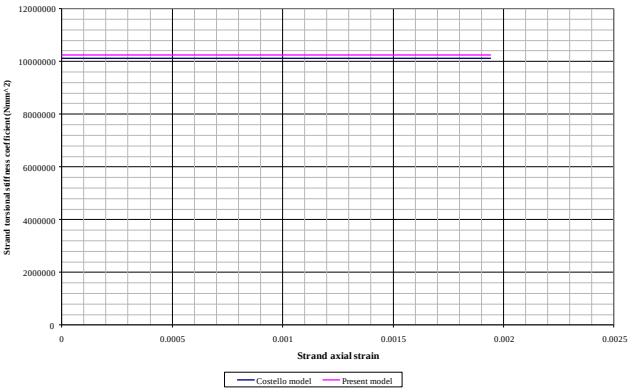

Fig. 9 Strand torsional stiffness coefficient

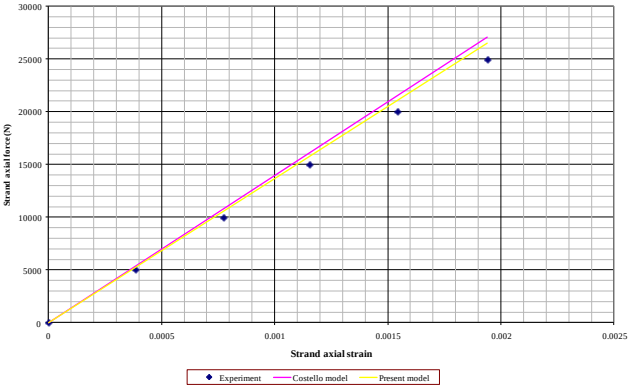

Fig 10 Strand axial force

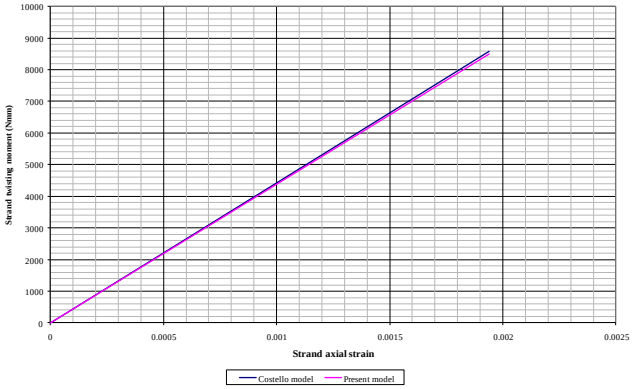

Fig. 11 Strand twisting moment

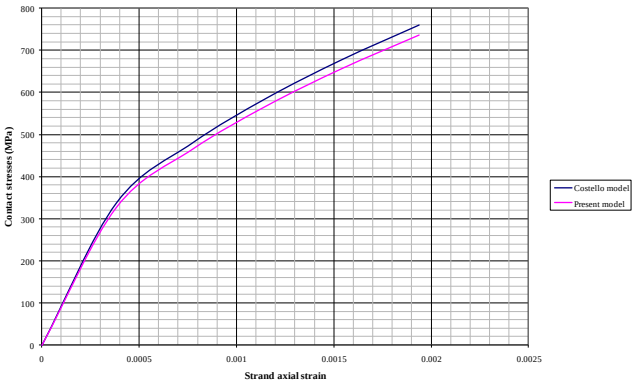

The experimental results generally agree with the results of the present model but registers about 4.8% increase in the strain ranges considered. This deviation is due to the role of the friction coefficient at the contact

ISBN: 978-988-19251-5-2
ISSN: 2078-0958 (Print); ISSN: 2078-0966 (Online)

interface. As the conditions of the friction coefficient in the experimental sample and the assumed value of friction coefficient in the present model are not exactly equal, the deviation in the experimental result is bound to be acceptable.

III. Conclusion

A new model has been developed to calculate the axial response of a single layered strand taking the frictional effects at the interface into account. A strand with lateral contact is analysed. The present work considered the inclusion of the frictional forces at the contact interface and has predicted the various parameters that contribute to the cable response. The analytical results of the present model, when compared with that of Costello and other similar researchers register deviation in the individual parameters, though the overall axial response is in agreement. The deviation of the results in the individual parameters is attributed to the consideration of tangential frictional forces and their associated moments.

From both the analytical results and the experimental findings, it is concluded that cable behaviour of the wire strand has an important role on the friction coefficient. It is hoped that the findings of the present work will help in the optimal design of stranded cables. The result can be useful to estimate the wear at metallic interfaces and further research in these directions are in progress.

Acknowledgment

The authors thank the Central Power Research Institute, Bangalore, India for providing laboratory facilities for the execution of the experiment.

References

[1] A. E. H. Love, A treatise on the mathematical theory of elasticity, Dover publishers, New York, 1944 pp.
[2] G. A. Costello, J. W. Phillips, Contact stresses in thin twisted rods, Journal of Applied Mechanics 40 (1973) 629 – 630.
[3] J. W. Phillips, G. A. Costello, Contact stresses in twisted wire cables, Journal of Engineering Mechanics, 99 (1973) 331-341.
[4] G. A. Costello, J. W. Phillips, A more exact theory for twisted wire cables, Journal of Engineering Mechanics, 100 (1974) 1096-1099.
[5] G. A. Costello, J. W. Phillips, Effective modulus of twisted wire cables, Journal of Engineering Mechanics, 102 (1976) 171-181.
[6] G. A. Costello, K. S. Sinha, Torsional stiffness of twisted wire cables, Journal of Engineering Mechanics, 103 (1977) 766-770.
[7] G. A. Costello, Theory of wire rope, Springer Verlag, Newyork, Berlin Heidelberg, 1990, pp. 11-43.
[8] K. Kumar, J. E. Cochran, J. A. Cutchins, Contact stresses in cable due to tension and torsion, Journal of Applied Mechanics, 64 (1997) 935-939.
[9] B. K. Gnanavel, D. Gopinath, N. S. Parthasarathy, Effect of friction on coupled contact in a twisted wire cable, Journal of Applied Mechanis, 77 (2010) 1-6.
[10] B.K. Gnanavel, N. S. Parthasarathy, Effect of interfacial contact forces in radial contact wire strand, Archive of Applied Mechanics, 81(2011) 303–317.

Nomenclature

E Young's modulus of the core and the helical wire, N/mm^2
F_ε Axial stiffness coefficient, N
F_χ Tension – torsion stiffness coefficient, Nmm
F_c Axial force of the core, N
F_w Axial force of the wire, N
F Axial force of the strand, N
G' Bending moment of the wire along the binormal direction, Nmm
H Wire twisting moment along axial direction, Nmm
h_0 Initial strand length, mm
K Distributed wire unit moment about normal direction of wire, Nmm/mm
K' Distributed wire unit moment about binormal direction axis of wire, Nmm/mm
l_0 Initial length of the helical wire, mm
M_w Wire twisting moment about strand axial direction, Nmm
M_ε Torsion – tension coupling stiffness coefficient, Nmm
M_χ Torsional stiffness coefficient due to axial load Nmm^2
M_c Twisting moment of the core, Nmm
m Number of the wire
N, N' Wire force along the normal and binormal direction, N
P, Q Tangential distributed force between wire to wire contacts, N/mm
R_{w0} Undeformed radius of helical wire, mm
R_{c0} Undeformed radious of the core, mm
r_0 Initial helical radious, mm
T Axial force of the helical wire, N
X, Y, Z Distributed wire unit force in normal, binormal axial direction, *N/mm*
Θ Distributed wire unit moment in axial direction, Nmm/mm
$\tau_0, \Delta\tau$ Intital and change in twist of the helical wire, rad/mm
$\kappa_0', \Delta\kappa'$ Initial and change in binormal curvature, rad/mm
α_0 Initial helix angle, Degree
μ Coefficient of friction
ν Poisson's ratio
$\frac{d\chi}{h}$ Angle of twist per unit length of the strand, rad/mm
ε Strand axial strain
σ_{w-w} Normal contact stress, Pa
χ Angle of outering sweep out in a plane perpendicular to the axis of the strand, Degree
ε_w Helical wire axial strain

ISBN: 978-988-19251-5-2
ISSN: 2078-0958 (Print); ISSN: 2078-0966 (Online)